Theoretical Study of NCO and RCCH (R = H, CH_3, F, Cl, CN) [3 + 2] Cycloaddition Reactions

Hsin-Tsung Chen and Jia-Jen Ho*

Department of Chemistry, National Taiwan Normal University, 88, Section 4, Tingchow Road, Taipei, Taiwan 117

Received: May 6, 2003; In Final Form: July 11, 2003

We carried out a theoretical study of the radical [3 + 2] cycloaddition reaction of NCO + RCCH (R = H, CH_3, F, Cl, CN), which produced a five-membered ring heterocyclic oxazole. An asynchronous two-bond formation mechanism was found, which led to a certain regioselectivity in the products when the substituted alkyne was used as a reactant. The preferable reactive sites of RCCH in various substituents are calculated by employing the Fukui functions and HSAB theory, and the results are in good agreement (except R = F) with the calculated energy barriers of the transition states in the potential energy surfaces. The N atom of NCO attacks the unsubstituted carbon atom of RCCH first, followed by the ring closure of the O atom with the other carbon atom to form the substituted oxazole. The order of the calculated first transition barriers (uts1) in the substituted alkynes (RCCH) is R = H > F > CN > Cl > CH_3, and that for the second transition barriers (uts2), R = H > CH_3 > CN > Cl > F. The reason for the decreased transition barriers of the substituted alkynes is analyzed.

Introduction

A number of oxazole-containing products continue to attract interest, and they are important in synthesis[1] and in biology.[2] For instance, they are used as auxiliaries in the form of latent carboxylic acid group equivalents[3] (triamide, ester, w-cyano anhydride) and aza diene components in Diels−Alder reactions with acetylenes and alkenes[4] to give furans and pyridines in synthesis. The oxazole ring systems are common structural motifs in a number of biologically active molecules[5] in biology. These five-membered heterocyclic ring systems originate in nature as a consequence of peptide modifications containing serine, threonine, and cysteine side-chain residues and are the products of cyclodehydration and redox reactions.[6] The oxazole molecule may be formed via a [3 + 2] cycloaddition mechanism in the mixture of NCO plus RCCH. It is shown in Scheme 1 that this [3 + 2] cycloaddition is asynchronous, not like the Diels−Alder or 1,3-dipolar [3 + 2] cycloaddition reaction[7] in which the two-bond formation is concerted. On the contrary, it proceeds in two steps: first the addition of an NCO radical to a carbon of RCCH, giving rise to an intermediate, followed by a ring closure, finally yielding the oxazole radical.

Several previous theoretical studies on the polarizabilities and structure of oxazole have been reported.[8] In this paper, we studied theoretically a series of NCO addition reactions to several substituted alkynes to form substituted oxazoles and discussed the regioselectivity exhibited by this type of reaction. Although charge transfer and HOMO−LUMO interactions (frontier molecular orbital, FMO, approach) are commonly used to understand the regioselective nature of a reaction,[9] occasionally the validity of this simple approach is inadequate. Therefore, we also applied DFT (density functional theory) -based reactivity descriptors such as Fukui functions and local softness,[9,10] which were generally proved to be successful in the prediction and interpretation of regioselectivity in various types of electrophilic and nucleophilic reactions.[11−15]

Computational Methods

We carried out the quantum mechanical calculations by using the Gaussian 98 program package.[16] The stationary points on the potential energy surfaces for the NCO + RCCH reactions were optimized mainly by density functional theory with the Becke three-parameter hybrid method and the Lee−Yang−Parr correlation functional approximation (B3LYP).[17−18] Basis sets with increasing accuracy of polarized split-valence and diffuse functions for heavy and hydrogen atoms 6-31++G** were used in the calculations. Vibrational analysis was carried out at the same level of theory to characterize the optimized structures as local minima or transition states. Zero-point energy (ZPE) correction was performed at the B3LYP/6-31++G** level. To obtain more reliable energies, coupled cluster calculations with single and double excitations and an evaluation by the perturbation theory of triple contributions CCSD(T)[19] were carried out for those geometries optimized at the B3LYP/6-31++G** level, denoted as CCSD(T)/6-31++G**// B3LYP/6-31++G**. Intrinsic reaction coordinate (IRC)[20] calculations were also performed to confirm the connection between the transition state and the designated intermediates. The reason that we adopted this level and basis set was that we applied it to calculate the activation energy of a similar reaction of NCO + C_2H_6 → HNCO + C_2H_5, and it yielded a satisfactory result (3.68 kcal/mol, or 15.38 kJ/mol) in good agreement with the experimental data (15.2 ± 0.4 kJ/mol).[21] Therefore, we are confident of the data calculated at this level for this type of reaction. Atomic charges are calculated from natural population analysis (NPA) by using the NPA options in the program.

Results and Discussion

This section has three parts to describe the roles of the reactants, the structural variation, and the energetics of the

* Corresponding author. E-mail: jjh@scc.ntnu.edu.tw.

10.1021/jp035220o CCC: $25.00
Published on Web 08/26/2003

SCHEME 1

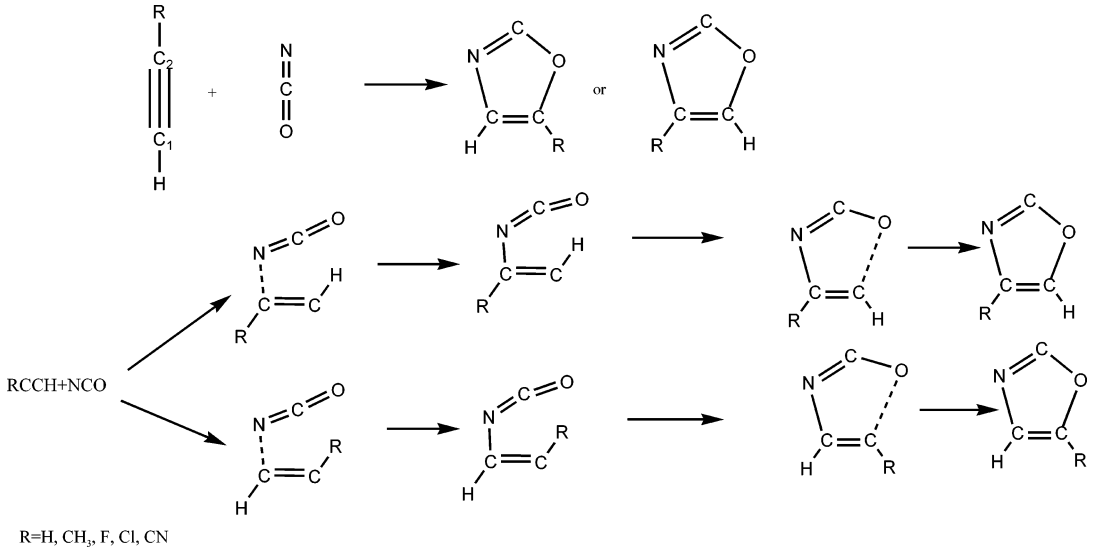

TABLE 1: Differences (in au) between HOMO and LUMO Energies of NCO and the Substituted Alkynes

structure	HOMO[a]	LUMO[a]	ΔE[HO(HCCR) − LU(NCO)]	ΔE[HO(NCO) − LU(HCCR)]
NCO	−0.34246[b]	−0.01441[b]		
HCCH	−0.29707	0.00391	0.28266	0.34637
HCC−CH_3	−0.27239	−0.00842	0.25798	0.33404
HCCF	−0.29698	−0.01245	0.28257	0.33001
HCC−Cl	−0.28385	−0.01117	0.26944	0.33129
HCC−CN	−0.32053	−0.07055	0.30612	0.27191

[a] Frontier orbital energies taken from the B3LYP/6-31++G** level. [b] The values of HOMO and LUMO are the MO energies of alpha (α) orbitals. The assignment of HOMO is π, and that of LUMO is σ.

species on the potential surfaces, the potential profiles, and the use of Fukui functions to explain the regioselectivity.

A. Roles of NCO and RCCH in the Reaction. Our first step in studying this reaction was to classify the roles of NCO and RCCH in the reaction. In Diels−Alder [4 + 2] or 1,3-dipolar cycloadditions, the alkene or alkyne was recognized as an electrophile, and the other reactant, diene or 1,3-dipole, as a nucleophile. However, we found a quite different result by applying FMO theory[22] to the NCO + RCCH reaction. The energies of both the HOMO and LUMO of NCO and RCCH (R = H, CH_3, F, Cl, and CN) were calculated, respectively, and the values of HOMO(NCO) − LUMO(RCCH) together with HOMO(RCCH) − LUMO(NCO) were evaluated. The data were shown in Table 1. It is clear that in almost every case of RCCH (except R = CN) the value of HOMO(RCCH) − LUMO(NCO) is smaller than the corresponding HOMO(NCO) − LUMO(RCCH) value. According to the frontier orbital theory, the HOMO of RCCH is more likely to interact with the LUMO of NCO because these two frontier orbitals are much closer as compared to the other pair. Therefore, the NCO molecule may provide the unoccupied orbital to RCCH and be considered as an electrophile, and the RCCH molecule, as a nucleophile. Furthermore, this tendency is more enhanced by the substitution of R (in RCCH) with an electron-donating group (such as CH_3). This effect may be understood as the electron-donating group enriching the electron density of HOMO and thus heightening the role of being a nucleophile of RCCH compared with an electron-withdrawing group (such as F, Cl, or CN). However, in any substituent (regardless of either electron-donating or -withdrawing properties, except for R = CN), the HOMO of RCCH is closer to the LUMO of NCO compared with the unsubstituted HCCH. To be certain of the roles of NCO and RCCH in the reaction, we also applied the Mulliken DA (donor−acceptor) theory.[23,24] As shown in the following drawing,

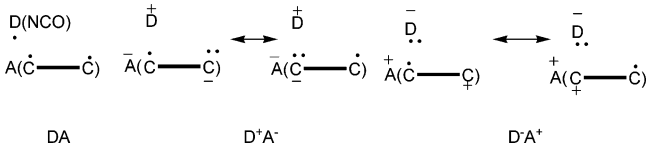

we arbitrarily denote the NCO radical as D and the alkyne as A. Thus, D^+A^- and D^-A^+ represent the charge-transfer configurations from D to A and A to D, respectively. We employed B3LYP/6-31++G** to calculate the adiabatic IE (ionization energy) and EA (electron affinity) for both NCO and RCCH, and the results are shown in Table 2. The corresponding experimental IEs of HCCH and HCC−CN, being 11.40 and 11.60 ev,[25] respectively, are also presented in parentheses as a comparison with the calculated values. The charge-transfer energies of D^+A^- and D^-A^+ are calculated as $D^+A^- = IE_{NCO} - EA_{RCCH}$ and $D^-A^+ = IE_{RCCH} - EA_{NCO}$, respectively. As shown in Table 2, the charge-transfer energies of D^-A^+ are much smaller than those of D^+A^-, which implies that the process of charge transfer from an alkyne molecule to NCO is more likely to occur. Besides, the scattering of the D^-A^+ values within a small range in the Table also reasonably represents the substitution effect from the substituted alkynes.

TABLE 2: Calculated Ionization Energies (IE)[a], Electron Affinities (EA)[a], and Charge-Transfer Energies Corresponding to the States (D^+A^- and D^-A^+)[b] of NCO Attack on the Unsubstituted Carbon Atom of HCCR[c]

structure	IE	EA	D^+A^-	D^-A^+
NCO	13.55	3.55		
HCCH	11.14 (11.40)[d]	−0.82	14.37	7.60
HCC−CH_3	9.97	−0.69	14.23	6.42
HCCF	11.02	0.10	13.45	7.48
HCC−Cl	10.31	0.44	13.11	6.76
HCC−CN	11.24 (11.6)[d]	0.42	13.13	7.70

[a] B3LYP/6-31++G** adiabatic ionization energies (IE) and electron affinities (EA) of NCO and alkynes in eV. [b] Charge-transfer energies of D^+A^- and D^-A^+ states calculated according to the following equations. $D^+A^- = IE_{NCO} - EA_{RCCH}$; $D^-A^+ = IE_{RCCH} - EA_{NCO}$. [c] D represents NCO, and A represents HCCR. [d] The corresponding experimental IEs of HCCH and HCC−CN, respectively, from ref 24.

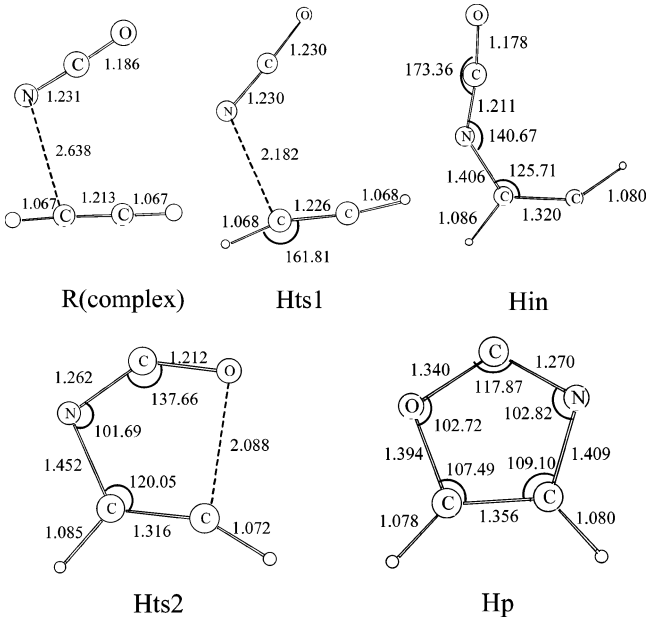

Figure 1. Calculated geometric structures of the transition states (Hts1, Hts2), intermediate (Hin), and product (Hp) of the NCO + HCCH reaction optimized at the B3LYP/6-31++G** level.

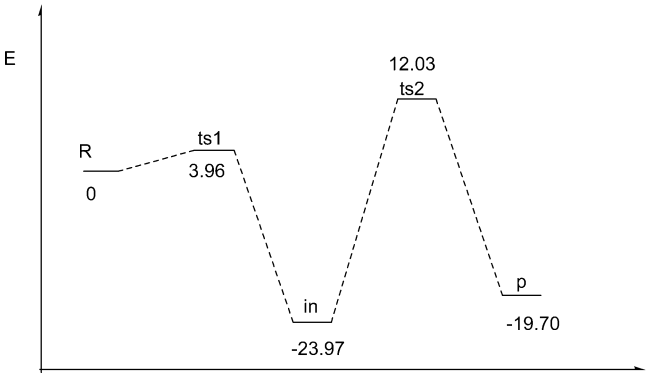

Figure 2. Schematic potential energy profile showing the two-step addition of NCO to HCCH. The relative energies (kcal/mol) are obtained at CCSD(T)/6-31++G**//B3LYP/6-31++G**.

An inspection of these data shows that it is satisfactory to believe that the NCO radical exhibits an electrophilic property toward the addition of RCCH.

B. Structural Parameters and Energetics Data. *1. NCO + HCCH.* The stationary geometries, including the reacting complex, transition states, and products, calculated at the B3LYP/6-31++G** level of theory are drawn in Figure 1. HR represents the reacting complex; Hts1, the first transition state; Hin, the intermediate; Hts2, the second transition state; and Hp, the final product (where H is added as a prefix to stand for unsubstituted alkyne HCCH). The relative potential energy diagram of each species calculated at CCSD(T)/6-31++G**//B3LYP/6-31++G** is drawn in Figure 2. Two-bond formation in this cycloaddition process is not synchronous, but one forms after the other. Each bond formation has one transition state (Hts1 or Hts2), and between the two transition states, there is one stationary intermediate (Hin). Because it acts like a radical addition, the NCO radical (where the unpaired electron is located primarily on the N atom) first attacks one of the carbon atoms of alkyne molecule by consuming 3.96 kcal/mol as an energy barrier to reach Hts1. The N···C distance decreases from 2.638 to 2.182 Å together with the increase in the carbon−carbon triple bond from 1.213 to 1.226 Å. After passing the barrier, a substantial heat of energy was released (ca. 24 kcal/mol) for a further decreased N···C distance to 1.406 Å associated with a further stretched C−C bond to 1.320 Å in Hin. The process may go on to form a five-membered ring heterocyclic product. In that case, it took about 36 kcal/mol for Hin to reach Hts2, but the net barrier is only 12.03 kcal/mol from the reacting complex (HR). The multiple bonds of both N−C and C−O in the NCO part of Hin were further stretched (N−C bond lengthens from 1.211 to 1.262 Å, and the C−O bond lengthens from 1.178 to 1.212Å) to gain the approach of the O···C distance to 2.088 Å in the second transition structure Hts2. The O···C distance keeps on approaching as well as the stretching of the C−C bond; finally the oxazole product (Hp) was reached, and a net heat of energy (ca. 20 kcal/mol) was released. We concluded that this cycloaddition reaction has a two-step mechanism: the N···C bond forms first, followed by the O··· C bond, which is quite different from the concerted two-bond formation in the Diels−Alder [4 + 2] and 1,3-dipolar cycloadditions.

2. NCO + HCC−CH$_3$ (Methyl Substitution). The substitution effect was studied. The calculated stationary geometries of the species on the potential energy surface were drawn in Figure 3, and the corresponded energy profiles, in Figure 4. We prefixed the letter M to R, ts1, ts2, and so forth to represent the methyl-substituted species. The existence of the substituent distinguishes the two carbons of the alkyne molecule, which provides the regioselectivity in this cycloaddition reaction. The NCO may either attack the methyl-substituted carbon and follow the path through Mts1, Min, and Mts2 to form Mp or strike the other unsubstituted carbon atom and subsequently pass through uMts1, uMin, and uMts2 finally to form uMp. u was prefixed to represent the species produced from the attack via the unsubstituted carbon atom. It is obvious from Figure 4 that there is regioselectivity; that is, NCO prefers to attack the unsubstituted carbon atom (barrier uMts1 < Mts1, uMts2 < Mts2). By comparing the structure of uMts1 and Mts1, we found that the N···C$_1$ bond length (2.226 Å) is longer than the N···C$_2$ bond length in Mts1 (2.133 Å) by 0.093 Å. Clearly, uMts1 is a transition structure at an earlier stage than Mts1, which means that uMts1 is closer to the reacting complex (MR). And according to the Hammond postulate, this process (via uMts1) would not only have a lower energy barrier but would also release more heat to reach the followed product. (uMin is more stable than Min.) A similar principle can be applied to the O···C$_2$ bond length in uMts2 (2.120 Å), which is longer than the O···C$_1$ bond length (in Mts2, 2.094 Å) by 0.026 Å; therefore, the barrier of uMts2 is smaller than that of Mts2, and that of uMp is also lower than that of Mp. By analyzing the first-stage transition structure of the unsubstituted alkyne (Hts1), we also found that the N···C bond length (2.182 Å) was shorter than the corresponding N···C$_1$ bond length in uMts1 (2.226 Å) by 0.044 Å and that in the second-stage transition structure the O···C bond length in Hts2 (2.088Å) was also shorter than the corresponding O···C$_2$ bond length in uMts2 (2.120 Å) by 0.032 Å, indicating that both transition structures uMts1 and uMts2 are situated at relatively earlier locations on the reaction coordinates than the corresponding Hts1 and Hts2, respectively. Therefore, this result might well (from the Hammond postulate) explain the outcome of smaller energy barriers in both first and second stages (by 2.44 kcal/mol, and 1.85 kcal/mol, respectively) of the approach of NCO to the unsubstituted carbon atom in the methyl-substituted alkyne than in HCCH.

3. NCO + HCCX (X = F, Cl, CN). The calculated stationary geometries on the potential surfaces are similar to those in Figure 3 with the methyl group replaced by the fluorine, chlorine, and

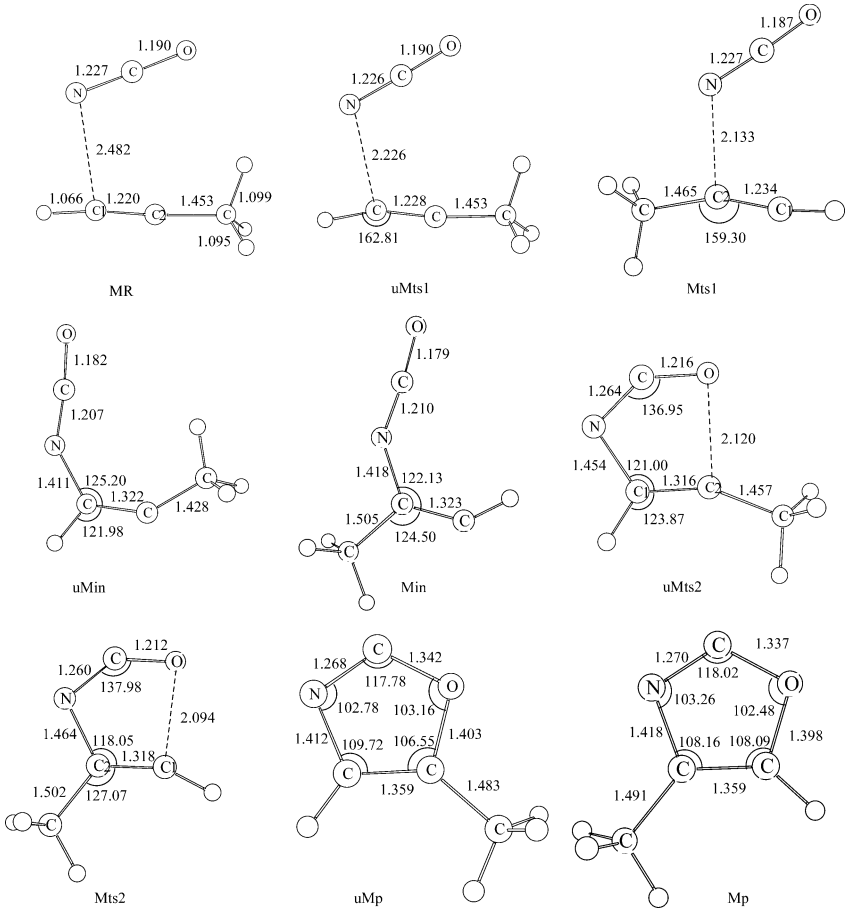

Figure 3. Calculated geometric structures of the transition states (uMts1, uMts2), intermediate (uMin), and product (uMp) for the attack of NCO on the unsubstituted carbon atom of HCCR. Those for the attack on the substituted carbon atom are symbolized as Mts1 and Mts2 (transition states), Min (intermediate), and Mp (product). All are calculated at the B3LYP/6-31++G** level.

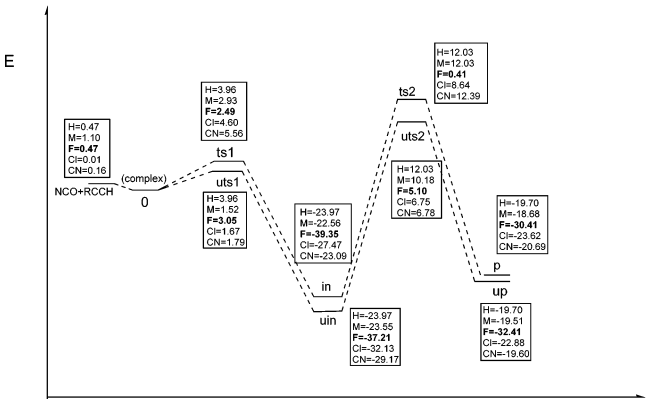

Figure 4. Calculated schematic potential energy profiles for the NCO + RCCH reaction, where R = H, M(CH_3), F, Cl, and CN. The relative energies (kcal/mol) are obtained at the CCSD(T)/6-31++G**//B3LYP/6-31++G** level.

cyanide group, respectively. All of the related structure parameters are listed in Table 3. These three different substituents show diverse regioselectivity in the process of cycloaddition. In fluorine substitution (HCCF), the NCO is more favorable to attack the substituted carbon atom. The relative energy barrier of ts1 (2.49 kcal/mol) is smaller than the uts1 (3.05 kcal/mol) shown in Figure 4. This is quite different from the other two substituents (Cl and CN) in which the NCO still prefers to attack the unsubstituted carbon atom. The energy barriers of ts1 in both Cl and CN are 4.60 and 5.56 kcal/mol, respectively; those in uts1 of Cl and CN are 1.67 and 1.79 kcal/mol. Obviously, the barriers increase by almost 3 times for NCO to attack the substituted carbon atom, but it is only about twice (2.93 in ts1 and 1.52 kcal/mol in uts1) in the methyl substituted alkyne. The N···C_1 distance (symbolized as r1 in Table 3) in uts1 of F substitution (2.247 Å) is shorter than that in ts1 (2.295 Å) by 0.048 Å; therefore, it obeys the Hammond postulate, and the transition energy of uts1 is a bit higher than ts1. The same parameters (r1) in both the Cl and CN substitutions of uts1 (2.290 and 2.243 Å, respectively) are much longer than those in ts1 (2.167 and 2.089 Å). As a consequence, the transition energy of uts1 in each case is much lower than that in ts1. A similar argument can be applied to explain the energy barriers of second transition states (uts2 and ts2) correlated to the O···C distance (symbolized as r6 in Table 3) in these three different substituents. The reason for the opposite outcome of transition energy in F substitution may be rationalized by the fact that in the transition structure of ts1 there is a strong repulsion between the fluorine atom and the nitrogen because of a much shorter C−F bond and much more intense charge density in the F atom as compared to that in the Cl- and CN-substituted counterparts. Therefore, the N···C distance may be longer in ts1(2.295 as compared to 2.247 Å in uts1), which means that ts1 is situated at an earlier location than the corresponding uts1 in their reaction coordinates. Beyond that, our NBO (natural bond orbital) calculation also revealed that there was a strong interaction (or back-donation, as you may call) between the lone-pair orbital (approximated to sp^2 character) of the F atom and the lone-pair orbital (unsaturated) of the C_1 atom (also approximated to sp^2 character), but it was not shown in the Cl- or CN-substituted counterpart. This interaction energy stabilized the ts1 more than the uts1 of the F-substituted alkyne, which was probably due

TABLE 3: Calculated Structural Parameters[a] of Stationary Geometries[b] of NCO + HCCR at the B3LYP/6-31++G Level**

	R(complex)					uts1					uin				
molecule	r1	r2	r3	r4	r5	r1	r2	r3	r4	r5	r1	r2	r3	r4	r5
HCCH	2.638	1.231	1.186	1.213	1.067	2.182	1.230	1.230	1.226	1.068	1.406	1.211	1.178	1.320	1.080
HCC-CH_3	2.482	1.227	1.190	1.220	1.453	2.226	1.226	1.190	1.228	1.453	1.411	1.207	1.182	1.322	1.428
HCCF	2.645	1.230	1.186	1.208	1.283	2.247	1.230	1.186	1.220	1.279	1.395	1.212	1.177	1.331	1.319
HCC-Cl	2.514	1.228	1.188	1.216	1.639	2.290	1.228	1.187	1.223	1.636	1.395	1.212	1.177	1.330	1.684
HCC-CN	2.617	1.230	1.185	1.213	1.372	2.243	1.231	1.183	1.226	1.365	1.391	1.218	1.172	1.319	1.329

	uts2						uP						ts1				
molecule	r1	r2	r3	r4	r5	r6	r1	r2	r3	r4	r5	r6	r1	r2	r3	r4	r5
HCCH	1.452	1.262	1.212	1.316	1.072	2.088	1.394	1.270	1.340	1.356	1.080	1.409	2.182	1.230	1.230	1.226	1.068
HCC-CH_3	1.454	1.264	1.216	1.316	1.457	2.120	1.412	1.268	1.342	1.359	1.483	1.403	2.133	1.227	1.187	1.234	1.465
HCCF	1.447	1.257	1.216	1.325	1.300	2.047	1.413	1.264	1.356	1.352	1.318	1.373	2.295	1.228	1.186	1.217	1.277
HCC-Cl	1.442	1.262	1.215	1.326	1.657	2.058	1.408	1.268	1.346	1.357	1.705	1.390	2.167	1.230	1.186	1.232	1.653
HCC-CN	1.420	1.270	1.216	1.335	1.361	2.000	1.396	1.273	1.333	1.367	1.410	1.402	2.089	1.234	1.182	1.237	1.388

	in					ts2						p					
molecule	r1	r2	r3	r4	r5	r1	r2	r3	r4	r5	r6	r1	r2	r3	r4	r5	r6
HCCH	1.406	1.211	1.178	1.320	1.080	1.452	1.262	1.212	1.316	1.072	2.088	1.394	1.270	1.340	1.356	1.080	1.409
HCC-CH_3	1.418	1.210	1.179	1.323	1.505	1.464	1.260	1.212	1.318	1.502	2.094	1.418	1.270	1.337	1.359	1.491	1.398
HCCF	1.384	1.212	1.174	1.315	1.351	1.422	1.259	1.211	1.323	1.334	2.081	1.384	1.277	1.332	1.356	1.328	1.400
HCC-Cl	1.387	1.211	1.175	1.315	1.760	1.438	1.260	1.211	1.320	1.731	2.080	1.399	1.273	1.336	1.358	1.718	1.395
HCC-CN	1.405	1.215	1.174	1.327	1.442	1.460	1.258	1.210	1.326	1.428	2.064	1.414	1.268	1.344	1.365	1.422	1.380

[a] The length unit is Å.

b

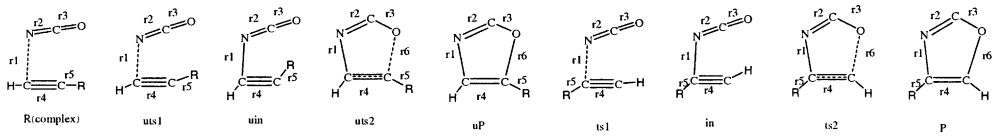

to the smaller dihedral angle of ∠CNCC in ts1, 15.8°, which is closer to 0° to enhance the interaction; howeer, it was 54.1° in uts1, which deviated further from a plane structure and hence decreased the orbital interaction.

C. Asynchronism in Addition. In this section, we apply the Fukui function[26] to prove the regioselectivity. The hard and soft acids and bases (HSAB) principle has been very useful in explaining the behavior of many chemical systems.[6−13] The extrapolation of the general behavior "soft likes soft" and "hard likes hard" locally, together with the idea that the larger the value of the Fukui function, the greater the reactivity, is also a very useful approach to explaining the chemical reactivity of a wide variety of systems.[27] Clearly, the determination of the specific sites at which the interaction between two chemical species is going to occur is of fundamental importance to the determination of the path and the products of a given reaction. The object of this part of the work is to introduce the Fukui function, to calculate the hardness and softness of an atom in a molecule, and to show through these quantities that a greater value of the Fukui function indeed implies greater reactivity and that the HSAB principle may be invoked as a criterion to determine the reactive sites of two interacting species. The Fukui function $f(r)$ is defined[10] either as the first derivative of the chemical potential (μ) with respect to the external potential $V(r)$ at a constant number of electrons N or as the first derivative of the electronic density $\rho(r)$ with respect to the number of electrons N at constant external potential $V(r)$.

$$f(r) = \left[\frac{\delta u}{\delta V(r)}\right]_N = \left[\frac{\partial \rho(r)}{\partial N}\right]_V$$

Because $\rho(r)$as a function of N has slope discontinuities, it provides the following three reaction indices.

$$f^-(r) = \left[\frac{\partial \rho(r)}{\partial N}\right]_V \quad \text{governing electrophilic attack}$$

$$f^+(r) = \left[\frac{\partial \rho(r)}{\partial N}\right]_V \quad \text{governing nucleophilic attack}$$

$$f^0(r) = \frac{1}{2}[f^+(r) + f^-(r)] \quad \text{for radical attack}$$

Yang and Mortier[28] later defined $f(r)$ in a more condensed form. The condensed Fukui functions of an atom, say k, in a molecule with N electrons are defined as

$$f_k^+ = [q_k(N+1) - q_k(N)] \quad \text{for nucleophilic attack}$$

$$f_k^- = [q_k(N) - q_k(N-1)] \quad \text{for electrophilic attack}$$

$$f_k^0 = \frac{[q_k(N+1) - q_k(N-1)]}{2} \quad \text{for radical attack}$$

where q_k is the electronic population of atom k in a molecule. In density functional theory, hardness (η) and softness (s) are defined as

$$2\eta = \left(\frac{\partial^2 E}{\partial N^2}\right)_V = \left(\frac{\partial u}{\partial N}\right)_V = \frac{1}{S}$$

TABLE 4: Condensed Fukui Functions for the N Atom in the NCO Radical and the Two Carbon Atoms in HCCR as Well as the Global and Local Softness of the Molecules Calculated at the B3LYP/6-31++G(d, p) Level

	f^{+a}			f^{-a}			f^{0a}			global softness	local softness $(s^0)^c$		
molecule	C_1	N	C_2	C_1	N	C_2	C_1	N	C_2	S[b]	C_1	N	C_2
NCO		0.536			0.575			0.555		2.721		1.511	
HCCH	0.113		0.113	0.430		0.430	0.272		0.272	2.275	0.618		0.618
HCC−CH_3	0.072		0.009	0.466		0.200	0.243		0.157	2.553	0.621		0.400
HCCF	0.312		0.417	0.476		0.287	0.394		0.352	2.490	0.981		0.877
HCC−Cl	0.340		0.052	0.415		0.119	0.378		0.034	2.756	1.041		0.093
HCC−CN	0.362		0.234	0.371		0.166	0.367		0.200	2.515	0.922		0.503

[a] The atomic charges are calculated using natural population analysis (NPA). [b] $S = 1/(\mathrm{IE} - \mathrm{EA})$. The energy unit is a.u. [c] $s^0 = f^0 \cdot S$.

where the global softness S is simply defined as the inverse of the global hardness η. The local softness $s(r)$ can be defined as

$$s(r) = \left(\frac{\partial \rho(r)}{\partial u}\right)_V$$

Therefore, $s(r)$ can be written as

$$s(r) = \left[\frac{\partial \rho(r)}{\partial N}\right]_V \left[\frac{\partial N}{\partial u}\right]_V = f(r) \cdot S$$

In our calculation for a system of N electrons, independent calculations were made for the corresponding $(N - 1)$, N, and $(N + 1)$ electron systems with the same geometry. A natural population analysis (NPA) yields $q_k(N - 1)$, $q_k(N)$, and $q_k(N + 1)$ for the predicted possible reacting sites of NCO and RCCH molecules, and the Fukui function is calculated as a difference in population between N and $N + 1$ or N and $N - 1$ electron systems. The result is listed in Table 4. The N atom in NCO emerges as the soft center, and the unsubstituted carbon atom (C_1) always appears at a much higher value of the calculated Fukui function in each substituted alkyne. We chose the f^0 value for comparison because the reaction is more characteristic of a radical addition. Gázquez et al.[26] pointed out in his derivation of the equation of interaction energy in terms of the local softness and the condensed Fukui function of an atom in the molecule that the largest value of the Fukui function is, in general, associated with the most reactive site. As a consequence, from our calculated data in Table 4, it is not too difficult to explain why the preferable reactive site usually occurs on the unsubstituted carbon atom (C_1) in most of the substituted alkynes, although the F-substituted one is an exception. However, the Fukui function of C_2, 0.352, is still competitive with that of C_1, 0.394. The possible explanation for this exception was raised in the previous section.

Summary

We have shown in this study the asynchronism of two-bond formation in [3 + 2] cycloaddition and the regioselectivity of radical attack on the substituted alkynes, which can be interpreted using DFT-based reactivity descriptors. The frontier molecular orbital theory also provides a good scheme for understanding the role of NCO, acting as an electrophile, in the reaction, which is different from the role of dienes or dipolar molecules as nucleophiles in Diels−Alder or 1,3-dipolar cycloaddition reactions. The calculated energy barrier of the second step in this two-step cycloaddition reaction is usually much larger than that of the first step. In addition, the energy barriers in both steps are smaller for the substituted alkynes compared with those of the unsubstituted counterpart.

Acknowledgment. Support for this research from the National Science Council of the Republic of China (NSC-91-2113-M-003-011) is gratefully acknowledged. We are also grateful to the National Center for High-Performance Computing, where the Gaussian package and computer time were provided.

References and Notes

(1) Reviews: Meyers, A. I. *Heterocycles in Organic Synthesis*; Wiley: New York, 1974.

(2) Kingston, D. G. I.; Kolpak, M. X.; LeFevre, J. W.; Borup-Grochtman, I. *J. Am. Chem. Soc*. **1983**, *105*, 5106. Meyers, A. I.; Amos, R. A. *J. Am. Chem. Soc*. **1980**, *102*, 870. Meyers, A. I.; Lawson, J. P.; Conver, D. R. *J. Org. Chem*. **1981**, *46*, 3119. Meyers, A. I.; Lawson, J. P.; Walker, D. G.; Linderman, R. J. *J. Org. Chem*. **1986**, *51*, 5111.

(3) Reviews and leading references: Wassermann, H. H.; Floyd, M. B. *Tetrahedron, Suppl*. **1966**, *7*, 441. Wassermann, H. H.; Gambale, R. J.; Pulver, M. J. *Tetrahedron* **1981**, *37*, 4059. Wassermann, H. H.; Ives, J. L. *Tetrahedron* **1981**, *37*, 1825. Wassermann, H. H.; McCarthy, K. E.; Prowse, K. S. *Chem. Rev*. **1986**, *86*, 845. Lipshutz, B. H.; Hungate, R. W.; McCarthy, K. E. *Tetrahedron Lett*. **1983**, *24*, 5155.

(4) For reviews of Diels−Alder reactions of oxazoles, see ref 1. Kompeiski, M. Y.; Florentev, V. L. Rms. *Chem. Rev*. (Engl. Transl.) **1969**, *38*, 540. Boger, D. L. *Tetrahedron* **1983**, *39*, 2869. Boger, D. L. *Chem. Rev*. **1986**, *86*, 781. Recent examples: Reddy, G. S.; Blatt, M. V. *Tetrahedron Lett*. **1980**, *21*, 3627.

(5) Lewis, J. R. *Nat. Prod. Rep*. **1999**, *16*, 389.

(6) Roy, R. S.; Gehring, A. M.; Milne, J. C.; Belshaw, P. J.; Walsh, C. T. *Nat. Prod. Rep*. **1999**, *16*, 249.

(7) (a) Gordon, M. D.; Alston, P. V.; Rossi, A. R. *J. Am. Chem. Soc*. **1978**, *100*, 5701. (b) Nguyen, L. T.; Proft, F. D.; Chandra, A. K.; Uchimaru, T.; Nguyen, M. T.; Geerlings, P. *J. Org. Chem*. **2001**, *66*, 6096−6103. (c) Nguyen, M. T.; Chandra, A. K.; Sakai, S.; Morokuma, K. *J. Org. Chem*. **1999**, *64*, 65−69.

(8) El-Bakali Kassimi, N.; Doerksen, R. J.; Thakkar, A. J. *J. Phys. Chem*. **1996**, *100*, 8752−8757.

(9) Fleming, I. *Frontier Orbitals and Organic Chemical Reactions*; Wiley: New York, 1976.

(10) Parr, R. G.; Yang, W. *J. Am. Chem. Soc*. **1984**, *106*, 4049.

(11) Yang, W.; Parr, R. G. *Proc. Natl. Acad. Sci. U.S.A*. **1983**, 82, 6723.

(12) Langenaeker, W.; Demel, K.; Geerlings, P. *J. Mol. Struct.: THEOCHEM* **1992**, *259*, 317.

(13) Langenaeker, W.; Demel, K.; Geerlings, P. *J. Mol. Struct.: THEOCHEM* **1991**, *234*, 329.

(14) Tielemans, M.; Areschka, V.; Colomer, J.; Promel, R.; Langenaeker, W.; Geerlings, P. *Tetrahedron* **1992**, *48*, 10575.

(15) Langenaeker, W.; Proft, F. De; Geerlings, P. *J. Phys. Chem*. **1995**, *99*, 6424.

(16) Frisch, M. J.; Trucks, G. W.; Schlegel, H. B.; Scuseria, G. E.; Robb, M. A.; Cheeseman, J. R.; Zakrzewski, V. G.; Montgomery, J. A.; Stratmann, R. E., Jr.; Burant, J. C.; Dapprich, S.; Millam, J. M.; Daniels, A. D.; Kudin, K. N.; Strain, M. C.; Farkas, O.; Tomasi, J.; Barone, V.; Cossi, M.; Cammi, R.; Mennucci, B.; Pomelli, C.; Adamo, C.; Clifford, S.; Ochterski, J.; Petersson, G. A.; Ayala, P. Y.; Cui, Q.; Morokuma, K.; Malick, D. K.; Rabuck, A. D.; Raghavachari, K.; Foresman, J. B.; Cioslowski, J.; Ortiz, J. V.; Stefanov, B. B.; Liu, G.; Liashenko, A.; Piskorz, P.; Komaromi, I.; Gomperts, R.; Martin, R. L.; Fox, D. J.; Keith, T.; Al-Laham, M. A.; Peng, C. Y.; Nanayakkara, A.; Gonzalez, C.; Challacombe, M.; Gill, P. M. W.; Johnson, B.; Chen, W.; Wong, M. W.; Andres, J. L.; Gonzalez, C.; Head-Gordon, M.; Replogle, E. S.; Pople, J. A. *Gaussian 98*, Revision A.6; Gaussian, Inc.: Pittsburgh, PA, 1998.

(17) (a) Becke, A. D. *J. Chem. Phys*. **1993**, *98*, 5648. (b) Becke, A. D. *J. Chem. Phys*. **1992**, *96*, 2155. (c) Becke, A. D. *J. Chem. Phys*. **1992**, *97*, 9173.

(18) Lee, C.; Yang, W.; Parr, R. G. *Phys. Rev. B* **1988**, *37*, 785.

(19) Lee, T. J.; Scuseria, G. In *Quantum Mechanical Electronic Structure Calculations with Chemical Accuracy*; Langnoff, S. F., Ed.; Kluwer Academic Press: Dordrecht, The Netherlands, 1995.
(20) Gonzalez, C.; Schlegel, H. B. *J. Phys. Chem.* **1989**, *90*, 2154.
(21) Becker, K. H.; Geiger, H.; Schmidt, F.; Wiesen, P. *Phys. Chem. Chem. Phys.* **1999**, *1*, 5305−5309.
(22) Poblet, J. M.; Canadell, E.; Sordo, T. *Can. J. Chem.* **1983**, *61*, 2068.
(23) Wong, M. W.; Pross, A.; Radom, L. *J. Am. Chem. Soc.* **1994**, *116*, 6284.
(24) (a) Shaik, S. S.; Bar, R. *Nouv. J. Chim.* **1984**, *8*, 11. (b) Shaik, S. S.; Hiberty, P. C. *J. Am. Chem. Soc.* **1985**, *107*, 3089. (c) Shaik, S. S.; Hiberty, P. C.; Lefour, J. M.; Ohanessian, G. *J. Am. Chem. Soc.* **1987**, *109*, 363. (d) Shaik, S. S.; Canadell, E. *J. Am. Chem. Soc.* **1990**, *112*, 1446.
(25) Houk, N.; Sims, J.; Duke, R. E., Jr.; Strozler, R. W.; George, J. K. *J. Am. Chem. Soc.* **1973**, *95*, 7287.
(26) Gázquez, J. L.; Meńdez, F. *J. Phys. Chem.* **1994**, *98*, 4591.
(27) Parr, R. G.; Yang, W. *Annu. Rev. Phys. Chem.* **1995**, *46*, 701.
(28) Yang, W.; Mortier, W. J. *J. Am. Chem. Soc.* **1986**, *108*, 5708.